The EMBO Journal vol.5 no.11 pp.3045-3049, 1986

Localization of two chymotryptic fragments in the structure of renatured bacteriorhodopsin by neutron diffraction

Jill Trewhella[1], Jean-Luc Popot[2], Giuseppe Zaccaï[3] and Donald M.Engelman

Yale University, New Haven, CT 06511, [1]Los Alamos National Laboratory, Los Alamos, NM 87545, USA

[2]Permanent address: Collège de France and Institut de Biologie Physicochimique, F-75005 Paris, and [3]Institut Laue Langevin, 156X, F-38042 Grenoble Cédex, France

Communicated by R.Henderson

The structure of crystalline purple membrane reconstituted from purified bacteriorhodopsin (BR) chymotryptic fragments has been studied by neutron diffraction. In one of the samples studied, the fragment C-2, encompassing the first two predicted transmembrane segments, was prepared from deuterated purple membrane. The diffraction changes when the natural C-2 fragment is substituted by a deuterated one are analysed in terms of a seven-helix model for BR. The assignment of the labelled fragment to one end of the molecule placed new constraints on folding models for the protein.
Key words: proton pump/membrane protein structure/ *Halobacterium halobium*

Introduction

The natural occurence of bacteriorhodopsin (BR) as a two-dimensional array within the purple membrane (PM) bilayer has been the basis for many structural investigations. The 6-7 Å three-dimensional map, derived from electron diffraction intensities and electron microscope images of PM patches (Henderson and Unwin, 1975; Leifer and Henderson, 1983), strongly suggests that the polypeptide is folded into seven membrane spanning α-helices. Additional support is given to this proposal from knowledge of the amino acid sequence (Ovchinnikov *et al.*, 1979; Khorana *et al.*, 1979) and labelling and proteolysis studies, as well as energetic arguments (Ovchinnikov *et al.*, 1979; Engelman *et al.*, 1980, 1982; Ovchinnikov, 1982; Huang *et al.*, 1982). These data have been interpreted to give locations in the sequence for the seven membrane spanning segments. However, the lack of well-ordered, three-dimensional crystals and difficulties of electron microscopy approaches have, to date, limited the determination of the structure to a resolution of about 6.5 Å in three dimensions (Leifer and Henderson, 1983) and 3.5 Å in projection (see Henderson *et al.*, 1986, and references therein). These maps do not permit the identification of transmembrane segments with sequence segments. While several such assignments have been proposed (Engelman *et al.*, 1980, 1982; Agard and Stroud, 1982; Wallace and Henderson, 1982; Katre *et al.*, 1984; Seiff *et al.*, 1984, 1986), experimental data are insufficient at present to define unequivocally the correct folding model. Consequently, understanding the mechanism of action of this light-driven proton pump remains an important challenge (for a review, see Stoeckenius and Bogomolni, 1982).

Our approach to this problem has been to deuterate specifically known regions of the sequence and examine how well different assignment models predict the changes in the neutron diffraction pattern introduced by the deuteration. In earlier experiments, deuterated amino acids were biosynthetically incorporated into BR to give PMs in which various amino acid types were labelled throughout the molecule (Engelman and Zaccaï, 1980; Trewhella *et al.*, 1983). Predicted neutron intensity changes were calculated from models in which the seven membrane spanning sequence segments were folded as ideal α-helices. Different models were constructed by assigning these helices to specific axial locations (derived from the electron density map) and varying the rotational orientations of the helices about their axes (Trewhella *et al.*, 1983).

There are a number of difficulties associated with this approach. (i) The labels are scattered throughout the whole molecule, resulting in smaller relative intensity changes at low resolution than if the same scattering length difference were more concentrated. (ii) Given that the label is diffuse and that powder intensities are measured and not structure factors, difference Fourier maps are very noisy and do not reflect accurately differences in label weight between helices. A modelling procedure had to be developed. (iii) A very large set of models had to be tested ($7! \times 6^7 = 1.4 \times 10^9$ models, allowing for all helix assignments and 6-fold rotations of each helix), making a global search impossible. (iv) The model structure is approximate: transmembrane segments are modelled as ideal α_I-helices, and the rest of the molecule (~25%) is missing. In the present work, there are two major differences with the previous crystallographic strategy: the label is much larger and it is concentrated in only two transmembrane segments. This results in large intensity changes at low resolution. The analysis is simpler because the position of only two of the seven helices is critical in predicting the neutron diffraction pattern. Finally, because of the strength and size of the label, imperfections in the model should be of secondary importance.

In the accompanying report (Popot *et al.*, 1986) a new approach to deuteration of part of BR sequence is described. Crystalline PM was reconstituted starting from purified BR chymotryptic fragments. Fragment C-2 comprises amino acid residues 1-71, encompassing the first two putative transmembrane helices, while fragment C-1 comprises the rest of the molecule. Large samples suitable for neutron diffraction measurements were reconstituted in which C-2 originated either from a hydrogenated PM preparation (all-H sample) or from deuterated PM (part-D sample). X-ray diffraction by both samples and neutron diffraction by the all-H sample demonstrated that the BR lattice had reformed with identical unit cell dimensions and a unit cell content indistinguishable from native BR (Popot *et al.*, 1986). We report here on a comparative analysis of the neutron diffraction patterns of the all-H and part-D reconstituted samples.

Results

Table I and Figure 1 show the neutron intensity data collected from the all-H and part-D reconstituted PM samples, as well as those for native PMs. There are 21 measurable intensity peaks

Table I. Lorentz corrected intensity data with standard deviations

h,k	Native PM	All-H reconstituted PM	Part-D reconstituted PM
1,1	36 695 (886)	37 006 (400)	97 611 (560)
2,0	14 512 (688)	13 480 (264)	80 334 (501
1,2 + 2,1	9434 (824)	8456 (432)	31 724 (594)
3,0	640 (354)	977 (196)	14 302 (573)
2,2	7078 (440)	7504 (486)	9393 (603)
1,3 + 3,1	8212 (450)	8458 (504)	13 122 (657)
4,0	5474 (540)	5050 (560)	7869 (564)
3,2 + 2,3	5106 (548)	5898 (560)	12 754 (612)
4,1 + 1,4	12 265 (658)	12 452 (712)	13 399 (679)
5,0	6206 (642)	7301 (686)	6883 (764)
3,3	0 (634)	0 (610)	0 (651)
4,2 + 2,4	10 859 (745)	11 148 (711)	13 368 (942)
5,1 + 1,5	4176 (963)	4476 (293)	5525 (803)
6,0	0 (667)	0 (610)	0 (651)
4,3 + 3,4	34 885 (1304)	33 747 (931)	29 213 (905)
5,2 + 2,5	8665 (720)	7096 (675)	6583 (848)
6,1 + 1,6	4365 (821)	3674 (622)	2188 (836)
4,4	0 (768)	0 (610)	0 (836)
7,0 + 5,3 + 3,5	6942 (829)	8430 (720)	11 465 (831)
6,2 + 2,6	1022 (733)	2020 (552)	2064 (855)
7,1 + 1,7	6023 (1017)	5386 (656)	7321 (737)

Native and All-H data are scaled such that the sum of the intensities are equal, while Part-D data are scaled such that the sum of the intensities is twice that of the native.

arising from the BR lattice to a resolution of about 7 Å. These correspond to 34 independent reflections. The 1,0 reflection is not included in Table I as it cannot be measured reliably (see below). Since the samples consist of a stack of rotationally disordered sheets, they give a powder diffraction pattern in which *h,k* and *k,h* reflections are overlapped, though not equivalent in the P_3 symmetry of the lattice. There are large differences in relative intensities between the part-D and all-H data while the all-H and native data are very similar. A conventional residual factor of 6.9% was calculated between the all-H and native data.

Contamination of in-plane reflections

Reconstituted PM samples contain about 3-fold more *Halobacterium* lipids than native PM, which results in much more intense lamellar reflections (Popot *et al.*, 1986). These reflections fall at the same angle as some in-plane reflections and, as they arc around, they may have a non-negligible contribution to the in-plane diffraction pattern. A further source of difficulty is the phase transition of the lipid component, that depends on relative humidity and affects the degree of order of the protein lattice (see Popot *et al.*, 1986). We have explored, therefore, different humidity conditions, and varied the lamellar to in-plane intensity ratios by H_2O/D_2O exchange (results not shown), before settling on the most appropriate conditions for data collection.

The best data available for native PM were collected at 20°C in 76% relative humidity. These conditions were not satisfactory for the reconstituted samples, as shown by a 1,1 reflection which, in the reconstituted all-H sample, was 40% larger than in native PM. This became worse at higher relative humidity values. The best data set for the reconstituted all-H control was obtained in 32% relative humidity. There are no differences in relative intensities between native data sets in the whole relative humidity range from 100% to dry, provided the samples contain H_2O; hydration differences are reflected in the D_2O data (Zaccaï and Gilmore, 1979; Rogan and Zaccaï, 1981; Zaccaï, in preparation). The same is true for data from reconstituted samples beyond the 2,0 reflection. In order to achieve the best counting statistics, data beyond the 2,0 reflection collected at both humidities were combined. The D_2O/H_2O exchange experiments showed that the 1,0 reflections of the reconstituted samples were heavily contaminated by the lamellar first order, but that there was no contamination beyond. The 1,0 reflections were excluded, therefore, from the analysis.

Model calculations

The weight of the deuterium label gives rise to intensity differences that are too large for difference Fourier analysis and a model-building analysis was used to locate the deuterated fragment. The model was developed and discussed by Trewhella *et al.* (1983). It is made up of seven ideal α-helices and does not account for about one-quarter of the molecule, found in the extramembrane regions. Probably because of this, there are non-negligible differences, particularly for the 1,1 reflection, between the intensities observed and those calculated from the model, but the Fourier projection maps are very similar (Trewhella *et al.*, 1983).

Two different reliability factors *R* were determined to compare observed and calculated intensities. They gave essentially the same result. In a first approach, observed differences were calculated between the all-H and part-D reconstituted data. Intensity differences to a resolution of 8.5 Å were calculated for models classified according to the locations of the two deuterated helices. All possible sequence-to-structure assignment models were evaluated; the orientations of the deuterated helices about their axes were varied in 120° steps. The *R* factor ranges for each model reflect the effects of rotating the calculated helices and of permutating hydrogenated helices over their five positions and deuterated helices over their two positions. In calculations that included higher resolution data, it was found that the same models were selected for, but the spread in *R* values for a given class of models was somewhat greater (by 2−3%) and showed greater variations with helix orientations (not shown).

A second approach to the analysis was to compare observed and calculated intensities for the partly deuterated structure without reference to the all-H data. Modelling intensity differences, as in the first approach, has the advantage that some systematic errors will be reduced, but it gives rise to larger total percentage errors. Because of the high level of deuteration in this experiment (the total scattering density of the molecule is about double), intensity distributions for different models show very large changes, and modelling intensities for the part-D sample may be subject to fewer errors and thus give better discrimination. For this analysis, each model was evaluated as before, except that only the part-D data were used and the *R* factors were calculated from the differences between predicted and observed relative intensities rather than intensity differences (see Materials and methods). This approach yielded the same hierarchy of models as previously, with comparable *R* factors (not shown).

The analysis was performed with different weights given to the reflections. Two *R* factor sets are shown in Table II. They omit either the 1,0 or both the 1,0 and the 1,1 reflections from the analysis. For data sets omitting the 1,0 and 1,1 reflections, the best assignment model yielded by the model-building calculations (positions 1+7) gave *R* factors in the range 16−48%. The 'next best' models gave *R* values in the ranges 31−56% (6+7) and 34−60% (5+7). Searches with the 1,1 reflection included (the 1,0 reflection was always left out because of contamination) gave a poorer discrimination between helix pairs. In a search of 45 360 models with all possible helix permutations and 3-fold

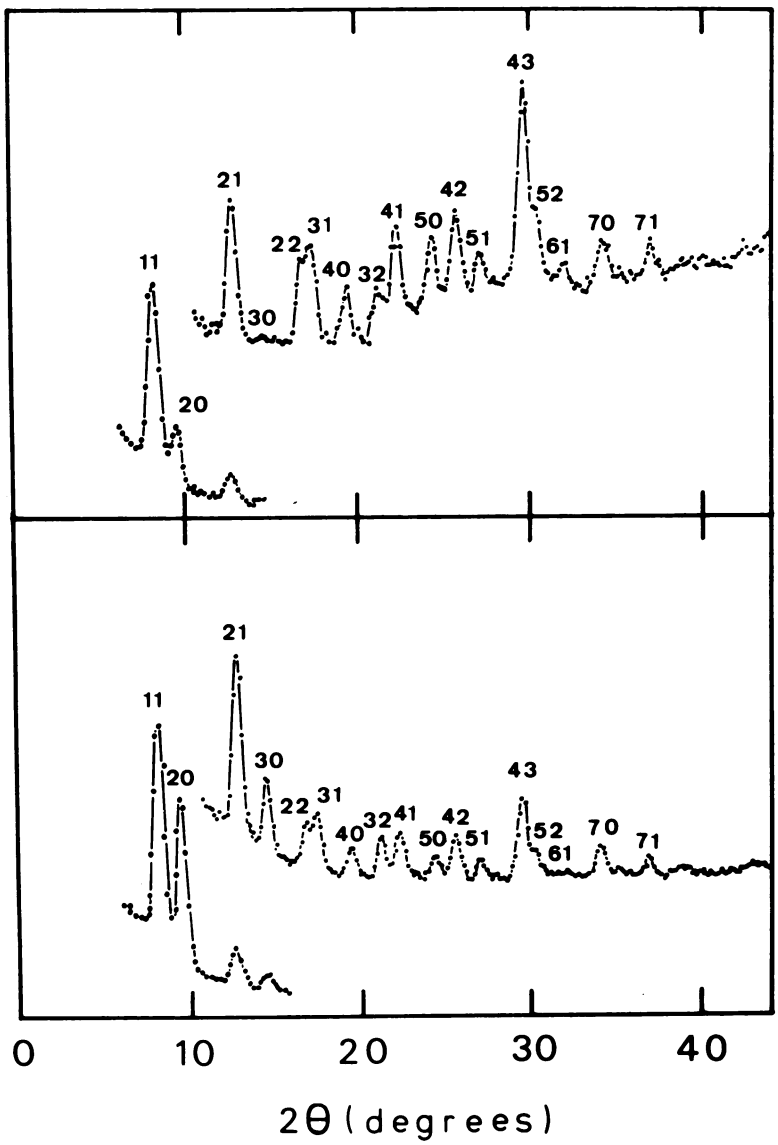

Fig. 1. Neutron diffraction patterns from the all-H reconstituted sample (top) and the part-D reconstituted sample (bottom). The low- and the high-angle parts of the patterns were collected independently (see text). From the 2,1 reflection onwards, the vertical scale has been expanded by a factor of 5. Scans are not scaled one to another. The figure incorporates only part of the data used to calculate intensity values given in Table I.

rotations of the two C-2 helices, all models with an R value below 35% had a labelled helix in position 7; the three combinations were 1+7 (R = 21−54%), 6+7 (R = 22−46%), and 4+7 (R = 32−57%). They all include neighbouring helices to 7 (helices 4 and 5 are very close to 7 of the adjacent molecule). The analysis is unambiguous therefore in placing the label on and around helix 7.

Discussion

The best models for the part-D data place the C-2 fragment in density position 7 and one of its neighbours in the structural map. R values for a given assignment of C-2 incorporate contributions from errors in the data and inadequacies in the model (in particular the missing linking regions). The C-2 fragment contains extra-membrane regions which are also deuterated, which will certainly lead to a larger label than the two model helices. The hierarchy of R values among models depends strongly on the weight given to the strong 1,1 and 2,0 reflections. When the 1,1 reflection is omitted, there is a marked preference for models with C-2 in positions 1 and 7. Omitting the 1,1 reflection might be justified by the fact that it is poorly predicted by the all-H model and because, being very much stronger than the other reflections, it tends to dominate the R factor calculations. Omitting both the 1,1 and the 2,0 reflections diminishes discrimination among models. These conclusions are not affected by changes in certain model assumptions such as displacing helix axes by a few ångstrøms (see Materials and methods) or varying the deuteration of C-2 used in modelling the part-D diffraction pattern from 80 to 100%.

Among the four possible assignments for the deuterated label giving the best agreement with observed data (positions 1+7, 6+7, 4+7 and 5+7), the 4+7 and 5+7 assignments have a larger R factor and do not appear very likely on structural grounds. Their relatively good fit to the data can be due to the proximity of helices 4 and 5 to helix 7 of a neighbouring molecule in the BR trimer (see Figure 2). The distance between helices 4 and 7 within a molecule appears to be large with respect to the number of residues available in order to bridge it (see Engelman *et al.*, 1980, 1982). In addition, it has been shown

Table II. *R* factors for the 21 possible assignments of C-2

Model Helix positions 1234567	*R* (%) *I*(1,1) to *I*(5,2)	*R* (%) *I*(2,0) to *I*(5,2)
**00000	77–103	95–126
*0*0000	83–108	76–96
*00*000	93–115	109–130
*000*00	105–137	91–124
*0000*0	71–109	86–110
00000	21–54	16–48
0**0000	71–91	89–112
0*0*000	76–97	95–119
0*00*00	92–124	110–139
0*000*0	76–101	92–122
0*0000*	51–82	57–93
00**000	53–83	68–98
00*0*00	59–92	42–78
00*00*0	58–89	58–87
00*000*	41–64	37–60
000**00	55–81	64–97
000*0*0	66–95	82–112
000*00*	32–57	39–70
0000**0	57–84	43–74
0000*0*	36–61	34–60
00000**	22–46	31–56

The positions occupied by the two deuterated helices (C-2) in the part-D sample are indicated by *. The *R* factors in the first column were calculated by using all reflections from 1,1 to 5,2; the 1,1 reflection was omitted in the calculation of the *R* factors in the second column.

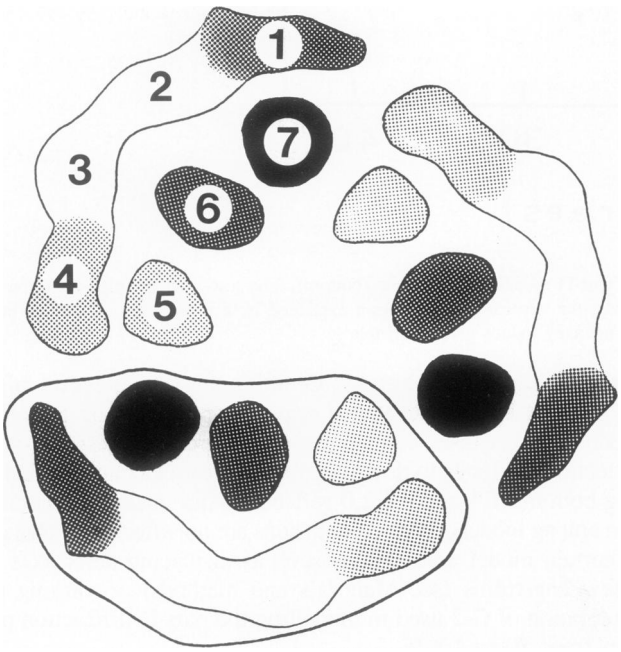

Fig. 2. A schematic representation of the probable C-2 assignments in BR structure. A protein trimer is shown, with the boundary of one of the BR molecules indicated (Unwin and Henderson, 1975; Leifer and Henderson, 1983). Positions are numbered according to Engelman *et al.* (1980). Shading densities reflect the probability for each position to be occupied by one of the two C-2 helices. The most probable assignments are 1+7 or 6+7 (see text).

that C-1 and C-2 fragments, after being separately refolded in distinct bilayers, can interact to regenerate BR (J.-L.Popot, S.-E.Gerchman and D.M.Engelman, submitted). This observation is more consistent with each fragment forming a compact region in the native structure. Although not definitive, these arguments strongly favour the C-2 helices occupying positions 1+7 or 6+7.

As previously (Trewhella *et al.*, 1983), we have based our analysis of the neutron diffraction data on the 7-α-helix model of BR (Henderson and Unwin, 1975). There is strong evidence to support such a model, but it is not universally accepted. An alternative proposal has been put forward, based mainly on spectroscopic evidence, in which the transmembrane domain of BR would comprise 5 α-helices and 4 β-strands (Jap *et al.*, 1983; Glaeser and Jap, 1985). Although this view is not generally shared among spectroscopists (cf. Mao and Wallace, 1984; Nabedryk *et al.*, 1985; Wallace and Teeters, 1986; see however Downer *et al.*, 1986), we would like to address the impact of such a model on our analysis and conclusions. The C-2 region of the sequence is predicted by both models to form two transmembrane α-helices, and there is direct evidence that the corresponding fragment takes up a highly α-helical structure on its own when reinserted into either lipid/detergent mixed micelles (Liao *et al.*, 1983) or lipid bilayers (J.-L.Popot, S.-E.Gerchman and D.M.Engelman, submitted). The structure assigned to this fragment therefore is not model-dependent. We have shown previously that the projection of the whole molecule calculated from the purely α-helical model is very similar, at 7 Å resolution, to the map derived from electron microscopy data (Trewhella *et al.*, 1983). This suggests that, at this resolution, whatever the secondary structure, the projected scattering density of the molecule is appropriately represented by the α-helical model for cases where the mean scattering density is uniform (i.e. for fully hydrogenated or uniformly deuterated structures). We consider, therefore, that our conclusions regarding the region of the molecule occupied by C-2 would remain valid even in the event of the presence of β-structure in the transmembrane domain of BR. It should be noted that the model of Jap *et al.* (1983) places β-strand in position 1. For the reasons mentioned above, the assignment of C-2 to positions 1+7 and such a model would be difficult to reconcile.

Figure 2 summarizes the information gained from the present neutron diffraction experiment on the folding of BR. Because the two C-2 helices are deuterated to the same extent, the experiment does not permit a separate identification of them. The assignment of these helices to position 7 and one of its neighbours places new constraints on possible folding models for BR. Unequivocal identification of the correct model, however, is not yet possible.

Materials and methods

Sample preparation

Two reconstituted PM samples were used in the course of this study. In both of them, the C-1 fragment and lipids originated from hydrogenated cultures. In sample no. 267 (designated *all-H*), the C-2 fragment was hydrogenated as well. In sample no. 272 (*part-D* sample), the C-2 fragment was purified from deuterated PM. The level of deuteration at non-exchangeable positions in the C-2 fragment was estimated to be approximately 85%. The preparation, characterization and diffraction properties of these two samples have been described in the preceding paper (Popot *et al.*, 1986).

Multilayered specimens were prepared by drying concentrated suspensions in K-buffer (KCl 150 mM, NaN_3 0.025%, K phosphate 6 mM, pH 6.0) on acid- and acetone-washed 0.025-mm-thick quartz slides. The all-H sample (95 mg protein) was spread over a 1 × 2 cm surface on the two sides of seven slides, the part-D sample (47 mg protein) over three slides. Both samples were partially dried by equilibration with either saturated $CaCl_2$ or saturated NaCl. The slides were mounted on the diffractometer perpendicular to the diffraction plane. Single slides were used for measurements of lamellar reflections due to membrane stacking. Mosaic spreads were about 20° full width at half-maximum. For measurements of in-plane diffraction, all the slides comprising a sample were stacked together.

Data collection

Neutron measurements were carried out on the D-16 diffractometer at the Institut Laue Langevin in Grenoble (see Jubb *et al.*, 1984). The sample was maintained at the indicated relative humidity by incubation with a saturated $CaCl_2$ or NaCl solution in a closed can. Neutrons of 4.52 Å wavelength were collimated by two vertical cadmium slits (4 × 30 and 3 × 20 mm), set 0.7 m apart. The two-dimensional ^3He detector positioned 1 m from the sample has an angular resolution of 0.145° horizontally. The sample was initially mounted with the planes of the slides perpendicular to the incident beam ($\omega = 0$) and data were collected in a modified $\omega/2\theta$ scan, with the ω setting equal to half the 2θ setting at the centre of the detector face in each position. Except for the 1,0 reflection, which was not used in the present analysis, the radius of the powder rings is sufficiently large as compared to the height of the detector face (80 mm) so that counts could be summed along vertical columns of detector elements without loss of angular resolution. Data collected at the same scattering angle for different positions of the detector were combined so as to average out differences in sensitivity. A Lorentz factor of $(h^2 + k^2 + hk)^{1/2}$ was applied to the observed intensities. The correction due to the differences in absorption and projection between the two extremes of a scan was negligible.

Modelling analysis

The modelling procedure has been described in detail in a previous publication (Trewhella *et al.*, 1983). Seven sequence segments, denoted A–G, have been assigned to the membrane-spanning segments of the polypeptide (Engelman *et al.*, 1980). These segments are an appropriate length to span the membrane and were identified by a combination of chemical modification and enzymatic digestion studies (see Engelman *et al.*, 1982; Dumont *et al.*, 1985; and references therein) as well as by energy calculations based on the free energy cost of burying a given amino acid sequence segment in the hydrophobic domain of the lipid bilayer (Engelman *et al.*, 1982). The sequence segments used were A: 7–1, B: 40–64, C: 77–101, D: 105–130, E: 134–158, F: 173–199 and G: 202–226.

Models were constructed by building each sequence segment as an ideal α_I-helix with amino acid side chains attached in standard configurations. The helix axes were then positioned according to the locations of the rods of density in the three-dimensional electron density map of Henderson and colleagues. In our earlier work, we used density maps kindly made available by Richard Henderson, that were based on observed electron diffraction intensity data and measured phases from electron microscope images to a resolution of 7 Å (Henderson and Unwin, 1975). For the present work, we also used density maps based on the work of Henderson and Agard, in which bacteriorhodopsin was modelled as seven ideal α-helices and the helix axis positions were refined against three-dimensional electron diffraction intensity data to 5 Å resolution (Henderson, private communication). The best agreement between the observed and calculated electron diffraction data (as evaluated by conventional residual factors) was obtained by assigning helices 1–4 to the locations obtained after refinement, and helices 5–7 to the original locations. This 'hybrid' model was used in some calculations, though the same rank ordering of models was obtained when analysis was done with either all the original axis locations or all the refined ones. Different models for testing were constructed by assigning particular sequence segments to specific density positions (assignment models) and varying the rotational orientations of individual helices about their axes (rotational models).

The observed intensity data were put on an absolute scale for comparison with the calculated data by applying a linear scale factor $\Sigma I_{ci}/\Sigma I_{oi}$ to the observed data, where I_{ci} and I_{oi} are the calculated and observed intensities respectively. This scale factor was calculated for each model. Models were assessed with the aid of a weighted residual defined as

$$R^2 = \frac{\sum_i \frac{1}{w_i}(X_{ci} - X_{oi})^2}{\sum_i \frac{1}{w_i}(X_{oi})^2}$$

where X_{oi} and X_{ci} are the observed and calculated intensity differences or intensities between two data sets and $w_i = \sigma_i^2 + K$. The standard deviation σ_i associated with each X_{oi} is calculated from counting statistics while K is a constant that approximates the systematic errors in the data (typically of the same order as the mean σ_i^2). Except for the strong 1,1 and 2,0 reflections, the weighting scheme was not critical; setting w_i equal to unity or σ_i (σ_i^2) did not affect the rank ordering of models. All the programs for the model building analysis were written in Fortran 77 to run on either VAX 11/750, VAX 8600 or IBM 3090/200 computers.

Acknowledgements

We thank R.Henderson for discussions and for communication of unpublished data, Lellis F.Braganza for help with data collection, M.Capel, Ph.Ledebt and the computer department of I.L.L. for their assistance with computing and the Centre Interrégional de Calcul Electronique (CIRCE) at Orsay for access to its computing facilities. This work was supported by grants AI20466 and GM22778 from the National Institutes of Health and grant PCM 8216854 from the National Science Foundation to D.M.E., grant F315/B04664 from the Office of Health and Environmental Research of the Department of Energy to J.T., C.N.R.S. grant 994043 from the Action Thématique Programmée 'Conversion de l'Energie dans les Membranes Biologiques' to G.Z. and long-term fellowships from the European Molecular Biology Organization and the Fondation pour la Recherche Médicale to J.-L.P.

References

Agard,D.A. and Stroud,R.M. (1982) *Biophys. J.*, **37**, 589–602.
Downer,N.W., Bruchman,T.J. and Hazzard,J.H. (1986) *J. Biol. Chem.*, **261**, 3640–3647.
Dumont,M.E., Trewhella,J., Engelman,D.M. and Richards,F.M. (1985) *J. Memb. Biol.*, **8**, 233–247
Engelman,D.M. and Zaccaï,G. (1980) *Proc. Natl. Acad. Sci. USA*, **77**, 5894–5898.
Engelman,D.M., Goldman,A. and Steitz,T.A. (1982) *Methods Enzymol.*, **88**, 81–88.
Engelman,D.M., Henderson,R., McLachlan,A.D. and Wallace,B.A. (1980) *Proc. Natl. Acad. Sci. USA*, **77**, 2023–2027.
Glaeser,R.M. and Jap,B.K. (1985) *Biochemistry*, **24**, 6398–6401.
Henderson,R. and Unwin,P.N.T. (1975) *Nature*, **257**, 28–32.
Henderson,R., Baldwin,J.M., Downing,K.H., Lepault,J. and Zemlin,F. (1986) *Ultramicroscopy*, in press.
Huang,K.-S., Radhakrishnan,R., Bayley,H. and Khorana,H.G. (1982) *J. Biol. Chem.*, **257**, 13616–13623.
Jap,B.K., Maestre,M.F., Hayward,S.B. and Glaeser,R.M. (1983) *Biophys. J.*, **43**, 81–89.
Katre,N.V., Finer-Moore,J., Stroud,R.M. and Hayward,S.B. (1984) *Biophys. J.*, **46**, 195–204.
Khorana,H.G., Gerber,G.E., Herlihy,W.C., Gray,C.P., Anderegg,R.J., Nihel,K. and Biemann,K. (1979) *Proc. Natl. Acad. Sci. USA*, **76**, 5046–5050.
Leifer,D. and Henderson,R. (1983) *J. Mol. Biol.*, **163**, 451–466.
Liao,M.-J., London,E. and Khorana,H.G. (1983) *J. Biol. Chem.*, **258**, 9949–9955.
Mao,D. and Wallace,B.A. (1984) *Biochemistry*, **23**, 2667–2673.
Nabedryk,E., Bardin,A.M. and Breton,J. (1985) *Biophys. J.*, **48**, 873–876.
Ovchinnikov,Yu.A. (1982) *FEBS Lett.*, **148**, 179–191.
Ovchinnikov,Yu.A., Abdulaev,N.G., Feigina,M.Yu., Kiselev,A. and Lovanov,N.A. (1979) *FEBS Lett.*, **100**, 219–224.
Popot,J.-L., Trewhella,J. and Engelman,D.M. (1986) *EMBO J.*, **5**, 3039–3044.
Rogan,P.K. and Zaccaï,G. (1981) *J. Mol. Biol.*, **145**, 281–284.
Seiff,F., Wallat,I., Ermann,P. and Heyn,M.P. (1985) *Proc. Natl. Acad. Sci. USA*, **82**, 3227–3231.
Seiff,F., Wallat,I., Westerhausen,J. and Heyn,M.P. (1986) *Biophys. J.*, in press.
Stoeckenius,W. and Bogomolni,R.A. (1982) *Ann. Rev. Biochem.*, **52**, 587–616.
Trewhella,J., Anderson,S., Fox,R., Khan,S., Engelman,D.M. and Zaccaï,G. (1983) *Biophys. J.*, **42**, 233–241.
Unwin,P.N.T. and Henderson,R. (1975) *J. Mol. Biol.*, **94**, 425–440.
Wallace,B.A. and Teeters,C.L. (1986) *Biochemistry*, in press.
Wallace,B.A. and Henderson,R. (1982) *Biophys. J.*, **39**, 233–239.
Zaccaï,G. and Gilmore,D. (1979) *J. Mol. Biol.*, **132**, 181–191.

Received on 25 July 1986